# Stress Corrosion Cracking of Welded Joints in High Strength Steels

*Variables affecting stress corrosion cracking are studied and conditions recommended for welding and postweld heat treat to obtain maximum resistance to cracking*

BY T. G. GOOCH

ABSTRACT. High strength steels may suffer a form of stress corrosion cracking (SCC) due to hydrogen embrittlement, the hydrogen being liberated by a cathodic corrosion reaction. Most service media will be expected to liberate hydrogen, and the problem affords a considerable drawback to the widespread use of high strength steels. For a number of reasons, failure may be particularly likely when welding is used for fabrication. Unless the structure is efficiently stress relieved, tensile stresses of yield or proof stress magnitude can remain in the vicinity of the weld, while even with stress relief, a weld will constitute a region of stress concentration. During the welding cycle, metallurgical changes may take place causing local microstructures that are particularly sensitive to SCC. The present investigation was initiated to clarify the situation, three particular objectives being identified, namely:

1. To define the relative SCC behavior of a range of high strength steels.
2. To assess the effects of welding and postweld heat treatment on SCC susceptibility.
3. To evaluate the general practical implications of the data obtained.

A range of steels was studied including both conventional medium carbon, low alloy materials and low carbon, precipitation hardening grades. SCC testing was based on linear elastic fracture mechanics principles using precracked specimens. Testing was carried out in 3% sodium chloride solution as representative of the media causing SCC of high strength steels. Welds were prepared in the experimental alloys and the pre-existing crack located in various regions of the joint, while samples were also prepared using The Welding Institute weld thermal simulator to reproduce specific heat-affected zone (HAZ) microstructures. Susceptibility was defined in terms of the critical threshold stress intensity to cause cracking, the results obtained being related to material composition and microstructure with reference to different heat affected zone and weld metal areas. Fractographic examination was carried out and susceptibility related to failure mechanism.

From the results obtained it has been possible to derive a general understanding of the variables affecting weld SCC performance. Susceptibility is primarily dependent upon microstructure, and, for a given material, recommendations may be made regarding welding conditions and postweld heat treatment to obtain maximum SCC resistance. The presence of twinned martensite in particular should be avoided, since this phase has a highly deleterious effect on SCC resistance. Provided postweld heat treatment similar to that specified for base metal is applied, HAZs and matching composition weld metals will generally show SCC resistance similar to the base metal; without such heat treatment, increased susceptibility must be anticipated. The presence of segregation and inclusions generally has little detrimental effect on weld metal SCC resistance, although segregation may be particularly significant in precipitation hardening systems. SCC failure may take place intergranularly, by cleavage, or by microvoid coalescence, intergranular failure being largely associated with the presence of twinned martensite and high susceptibility. The results suggest that highest SCC resistance will be obtained from low carbon, low alloy systems, since these are unlikely to suffer the development of deep corrosion pits which may act to initiate SCC in service, and will have high resistance to SCC by a cleavage mechanism.

Attention has been further paid to the practical risk of SCC initiation in service, consideration being given to the effects of environment on SCC initiation and propagation. A preliminary correlation has been obtained between fracture mechanics data and the SCC behavior of uncracked, undressed welds.

The information reported thus constitutes a rational basis for understanding the SCC behavior of welded joints. Although direct testing is still necessary to establish the behavior of a given joint in a particular environment, it is possible to maximize SCC resistance in advance by attention to relevant factors.

*T. G. GOOCH is Group Leader — Austenitic Group, The Welding Institute, Abington, Cambridge, Great Britain.* *Paper was presented at the 55th AWS Annual Meeting held in Houston during May 6-10, 1974.*

## Introduction

While it is widely realized that ferritic steels may be subject to stress corrosion cracking (SCC) in certain specific environments such as caustic conditions (Ref. 1), the environments causing trouble have in the past been relatively few and the problem has

not been widespread. However, during evaluation of high strength alloys (yield stress > 1000 N/mm²(150 ksi)) for aerospace and other applications, it became apparent that these materials could suffer a more general form of SCC in a variety of media at around room temperature, cracking arising in environments that had proved entirely innocuous in the past with lower strength alloys (Ref. 1). The reason for this susceptibility has been studied, and two hypotheses propounded, namely that failure is due either to the presence of a readily corrodible "active path" within the material, or to a form of hydrogen embrittlement, with the hydrogen being liberated by a cathodic corrosion reaction (Ref. 2). While the former mechanism may be operative in some instances, research has indicated that in general failure takes place as a result of hydrogen embrittlement (Ref. 3). From investigations into the problem of hydrogen embrittlement of steels, the risk of SCC can be expected to increase with increasing material hardness, and the phenomenon assumes particular significance in the case of high strength alloys.

Stress corrosion failure at welded joints in high strength steels may be especially likely for a number of reasons (Ref. 4). Unless the fabrication is efficiently stress relieved after welding, residual welding stresses will remain. In the weld area, these stresses will be tensile, and as they will normally be of yield stress magnitude, they can greatly increase the risk of cracking. Even with stress relief treatment, local stress concentrations at welds will usually remain. Depending on detail design, welded joints may be associated with crevices where concentration of aggressive chemical species can occur, further increasing the likelihood of failure. Metallurgical changes taking place during the welding thermal cycle may result in local microstructures that are particularly susceptible to SCC. Hence, SCC can occur at welded joints even though the base metal is relatively immune.

Despite a general appreciation of these factors, there is little information available regarding the SCC behavior of welds in high strength steels. Although a number of evaluation studies have been carried out relevant to specific alloys welded using particular techniques, the relative importance of the various factors determining weld performance has not been defined. In consequence, it has been difficult to make general recommendations for the avoidance of SCC in service. This lack of knowledge constitutes a potential drawback to the more widespread use of welded medium and high strength steels, especially since a very wide range of environments has been reported to cause cracking (Ref. 5). The present investigation was undertaken to clarify the situation, three particular objectives being identified:

1. Evaluation of the relative SCC behavior of a range of high strength steels.
2. Definition of the effects of welding and postweld heat treatment on SCC susceptibility.
3. Assessment of the general practical implications of the data obtained.

## Experimental Approach

Five high strength steels were selected as a basis for study, including both medium carbon, low alloy material and low carbon, precipitation hardening grades. The alloys chosen were FV520S, NCMV, RS140, 18% nickel maraging, and a copper-silicon steel Table 1, first five items), with the materials supplied as 25 mm (1 in.) and 15 mm (0.6 in.) thick plate (Ref. 6). Other, lower strength alloys were used in the course of the investigation to clarify certain aspects of SCC behavior (Table 1, last two items).

The program was carried out in two stages. First, welds were prepared in the experimental steels, and the SCC resistance of the various regions of these welds defined, comparison being made with base metal behavior. A linear elastic fracture mechanics approach to SCC testing was adopted, since the use of precracked samples reproduces the worst practical case of cracking initiating from a pre-existing welding defect, while the approach gives quantitative data of practical application (Ref. 7). Further, the crack can be sited in any region of a weld, and the risk of failure of individual weld regions assessed largely independently of surrounding material. Concurrently with these studies, metallographic and fractographic examination was carried out to identify the factors determining SCC behavior.

Second, SCC testing of plain uncracked welds was undertaken, and the results correlated with the fracture mechanics data. Compositional and microstructural gradients across an unmachined, uncracked weld may modify SCC initiation and propagation as compared to a precracked specimen where the development of SCC is largely controlled by the preexisting crack and associated plastic zone. Further, there is little information on the extent to which geometrical stress and strain concentrates at weld toes affect the corrosion processes causing SCC initiation. Thus, it was considered necessary to establish that relative data obtained from precracked samples were directly applicable to practice.

## Precracked Sample Studies

### Sample Preparation

The base metals were heat treated as in Table 2. Single edge notched and fatigue cracked (SEN) samples (Ref. 7) were machined as in Fig. 1, with adequate dimensions in all cases to give plane strain conditions during SCC testing, although this was not always the case with toughness tests in air (Ref. 8).

Welds were made in each steel to cover a range of processes of industrial application as indicated in Table 3. Matching composition filler metals were used in most cases, although consistent with normal practices, an FV520B filler metal was adopted for the FV520S GTA welds. In addition, a lower strength Ni-Mo-V filler metal was used for a GMA weld in NCMV steel. The weld metals studied are shown in Table 4.

A K-preparation (double-bevel-groove joint) was used for the arc welds to obtain an approximately planar fusion boundary and HAZ, so that the pre-existing crack could be located in any particular weld area,

**Table 1 — Analyses of Steels Used [a]**

| Material | C | Si | Mn | Ni | Cr | Mo | Cu | V | Ti | Nb | Ca | B | Zr | Al | Co |
|---|---|---|---|---|---|---|---|---|---|---|---|---|---|---|---|
| Cu-Si | 0.37 | 1.7 | 0.9 | — | — | 0.12 | 1.75 | 0.23 | — | — | — | — | — | — | — |
| RS140 | 0.36 | 0.25 | 0.58 | 0.26 | 3.2 | 0.96 | — | 0.21 | — | — | — | — | — | — | — |
| FV520S | 0.07 | 0.45 | 1.26 | 5.57 | 15.3 | 1.73 | 1.7 | — | 0.15 | — | — | — | — | — | — |
| Maraging | 0.009 | 0.005 | 0.09 | 18.0 | — | 3.19 | — | — | 0.31 | — | 0.01 | 0.003 | 0.006 | 0.07 | 9.25 |
| NCMV | 0.45 | 0.80 | 0.47 | 1.74 | 1.32 | 0.94 | — | 0.25 | — | — | — | — | — | — | — |
| BS4360 | 0.19 | 0.01 | 1.4 | 0.01 | 0.01 | 0.02 | 0.04 | 0.01 | | 0.015 | | | | | |
| HY80 | 0.19 | 0.19 | 0.28 | 2.85 | 1.46 | 0.44 | | | | | | | | | |

(a) Analyses supplied by RARDE, except for BS4360 and HY80, which were analyzed at The Welding Institute.

with fatigue and stress corrosion crack propagation taking place through approximately constant material microstructure. The electron beam welds were close square-groove butt joints.

SEN samples were machined as in Fig. 2, with dimensions based on results obtained from base metal, and intended to give plane strain conditions during SCC testing. The tip of the pre-existing crack was aimed at the supercritical (transformed) or subcritical HAZ, or at the weld metal.

Simulated HAZ specimens were prepared to assess the effect of peak temperature reached in the HAZ, and to study the worst case likely to arise in practice of a single pass weld with no post-weld heat treatment. For comparative purposes BS968 (now identified as BS430, grade 50B or 50C) and HY80 materials were studied as representing low alloy materials which would not develop such high HAZ hardnesses on welding as the medium carbon steels. Samples 10×10×50 mm (0.4×0.4×2.0 in.) of the NCMV and HY80 steels were heat treated using a thermal simulator to reproduce the HAZ cycle created by SMA welding at 1 kJ/mm (25kJ/in.) with a 250 C preheat, maintained for 24 h after cycling. Peak temperatures of 1300 C and 1000 C were reproduced. To develop maximum simulated HAZ hardness, similar size samples of Cu-Si, RS140, FV520S, BS968 and HY80 steels were austenitized at 950 C, quenched in glycerine, and stored in liquid nitrogen prior to testing. These samples were then edge notched and fatigue cracked.

Postweld heat treatment was carried out as in Table 5. Some welds were tested in the as-welded condition to examine the effect on SCC behavior of tempering during multipass deposition.

**Table 2 — Heat Treatment of Experimental Steels**

| Steel | Heat treatment [a] | Mechanical properties: Hardness [b] HV 20 | Yield stress [c] N/mm² | Yield stress [c] ksi |
|---|---|---|---|---|
| Cu-Si | 980 C, 1h OQ: T 350 C, 1h AC | 560 | 1490 | 220 |
| Cu-Si | 980 C, 1h OQ: T 600 C, 1h AC | 548 | 1370 | 200 |
| RS140 | 900 C, 1h OQ: T 350 C, 1h AC | 590 | 1310 | 190 |
| RS140 | 900 C, 1h OQ: T 600 C, 1h AC | 442 | 1150 | 170 |
| FV520S | 1050 C, 5 min AC: S 750 C, 2h AC: 20 C, 2h | 410 [d] | 1140 [d] | 165 |
| Maraging | 820 C, 1h OQ: PH 480 C, 3h AC | 408 | 1230 | 180 |
| NCMV | 920 C, 1h OQ: T 350 C, 1h AC | 460 | 1630 | 235 |
| NCMV | 920 C, 1h OQ: T 600 C, 1h AC | 407 | 1190 | 170 |

(a) OQ = Oil quenched to ambient temperature; AC = Air cooled to ambient temperature; T = Tempered; S = Sensitized; PH = Precipitation hardened
(b) Average of 10 determinations
(c) Average of 3 tests
(d) Tested in precipitation hardened condition, of further heat treatment 450 C, 2h AC

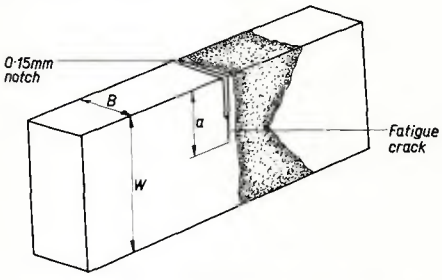


*Fig. 1 — Sketch of typical SEN specimen*

**Table 3 — Welding Conditions**

| Base Metal | Welding Process [a] | Plate Thickness, mm | Surfacing Passes: Voltage V | Current A | Speed mm/min | No. of passes | Final Weld: Voltage V | Current A | Speed mm/min | No. of passes | Preheat & Interpass Temp. C |
|---|---|---|---|---|---|---|---|---|---|---|---|
| Cu-Si | SMA [b] | 12.5 | 22 | 100 | NR | 1 | 22 | 100 | NR | 7 | 250 |
| RS140 | SMA [b] | 25 | 20 | 110 | NR | 4 | 20 | 110 | NR | 20 | 250 |
| RS140 | EB | 20 | NA | NA | NA | NA | $140\times10^3$ | $35\times10^{-3}$ | 250 | 1 | Room |
| FV520S | GTA [c] | 25 | 11 | 110 | 150 | 10 | 12 | 180 | 100 | 14 | Room |
| FV520S | EB | 25 | NA | NA | NA | NA | $140\times10^3$ | $35\times10^{-3}$ | 250 | 1 | Room |
| Maraging | SMA [d] | 25 | 22 | 140 | NR | 4 | 22 | 140 | NR | 18 | Room/100 |
| Maraging | GMA [e] | 25 | 20 | 200 | 460 | 3 | 20 | 200 | 460 | 11 | Room |
| Maraging | EB | 25 | NA | NA | NA | NA | $140\times10^3$ | $35\times10^{-3}$ | 250 | 1 | Room |
| NCMV | SMA [b] | 12.5 | 20 | 110 | NR | 1 | 20 | 110 | NR | 7 | 250 |
| NCMV | GMA [f] | 25 | 27 | 230 | 275 | 3 | 24 | 230 | 275 | 11 | 250/350 |

(a) SMA = Shielded metal-arc; GTA = Gas tungsten-arc; GMA = Gas metal-arc; EB = Electron Beam; NA = Not applicable; NR = Not recorded
(b) 3.2 mm diam electrodes
(c) 2.8 mm diam filler wire
(d) 4 mm diam electrodes
(e) 1.2 mm diam wire, Ar/2%$O_2$ shielding gas
(f) 1.6 mm wire, Ar/5%$O_2$ shielding gas

**Table 4 — Weld Metal Compositions**

| Base metal | Welding process | Element (wt %): C | S | P | Si | Mn | Ni | Cr | Mo | V | Cu | Nb | Ti | Al | B | Pb | Sn | Co |
|---|---|---|---|---|---|---|---|---|---|---|---|---|---|---|---|---|---|---|
| Cu-Si | SMA [a] | 0.42 | 0.014 | 0.030 | 1.57 | 1.05 | 0.05 | 0.06 | 0.21 | 0.28 | 1.47 | 0.01 | 0.03 | 0.016 | 0.001 | 0.01 | 0.02 | 0.02 |
| RS140 | SMA [a] | 0.29 | 0.010 | 0.024 | 0.08 | 0.25 | 0.38 | 3.16 | 2.16 | 0.16 | 0.08 | 0.005 | 0.01 | 0.010 | 0.001 | 0.01 | 0.01 | 0.01 |
| FV520S | GTA [b,c] | 0.06 | 0.01 | 0.02 | 0.25 | 0.8 | 5.9 | 14.3 | 1.7 | — | 1.6 | 0.25 | — | — | — | — | — | — |
| Maraging | GMA [d] | 0.03 | 0.006 | 0.004 | 0.10 | 0.05 | 17.7 | — | 4.04 | — | — | — | 0.26 | 0.08 | 0.003 | — | — | 8.0 |
| Maraging | SMA [d] | 0.03 | 0.013 | 0.002 | 0.15 | 0.08 | 17.9 | — | 3.33 | — | — | — | 0.14 | 0.08 | — | — | — | 8.4 |
| NCMV | SMA [a] | 0.59 | 0.012 | 0.025 | 1.04 | 0.36 | 2.55 | 1.91 | 1.39 | 0.29 | 0.07 | 0.005 | 0.03 | 0.011 | 0.001 | 0.01 | 0.01 | 0.02 |
| NCMV | GMA [c] | 0.07 | 0.01 | 0.01 | 0.5 | 1.35 | 1.3 | — | 0.45 | 0.15 | — | — | — | — | — | — | — | — |

(a) Weld metal analysis
(b) FV520B filler metal used
(c) Typical filler metal used
(d) Weld metal analysis carried out by International Nickel Co., apart from carbon

### Mechanical Testing

Hardness surveys were made on all base metals and welded joints. Yield stress values were obtained for base metals and weld metals. SEN samples were tested in 3 point bend in air and the relevant fracture toughness determined.

### SCC Testing

The precracked specimens were loaded in 3 point bend and exposed to a 3% NaCl solution, selected as representative of the media causing SCC of high strength steels (Ref. 9). The initially applied stress intensity was varied, and the time to failure recorded to determine the critical threshold stress intensity below which SCC would not take place. Studies were also undertaken using an incremental load technique, the rate of load increase being such that complete failure of the sample took place between increments, and the threshold stress intensity was not exceeded by any great margin. Testing was carried out until a reasonable indication of threshold behavior was obtained; with highly susceptible materials, this normally entailed tests of up to about 200 h, although testing on SCC resistant materials was carried out for up to 2000 h.

### Metallographic Examination

Optical metallography was carried out on all welds. Carbon extraction replicas and thin foils were prepared from the various regions tested, and examined in the electron microscope. Fractographic examination was carried out using the scanning electron microscope. The retained austenite contents of the experimental weld metals were determined by x-ray diffraction.

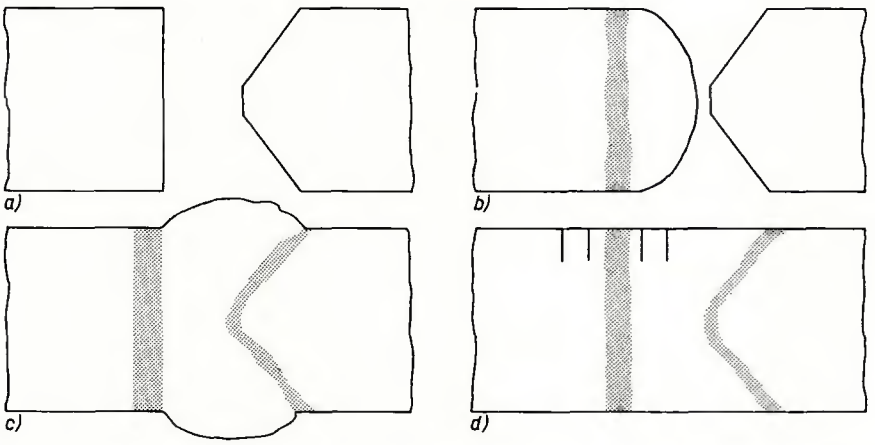


*Fig. 2 — K-preparation (double-bevel-groove) welding procedure: (a) joint preparation, (b) one side surfaced with filler metal, (c) joint completed and (d) joint machined and notched as required*

**Table 5 — Post Weld Heat Treatment Conditions and Weld Metal Yield Stress**

| Steel | Base metal heat treat condition | Weld | Post weld heat treatment | Weld Metal Yield stress N/mm²(ksi) |
|---|---|---|---|---|
| Cu-Si | T 350 C | SMA | T 350 C, 1h AC | 1500 (220) |
| Cu-Si | T 600 C | SMA | T 600 C, 1h AC | ND[a] |
| RS140 | T 350 C | SMA | T 350 C, 1h AC | ND |
| RS140 | T 600 C | SMA | None | ND |
| | | SMA | T 600 C, 1h AC | 920 (135) |
| RS140 | | EB | None | ND |
| RS140 | | EB | T 500 C, 1h AC | ND |
| FV520S | S 750 C | GTA | 750 C, 2h AC: 0 C, 2h: PH 450 C, 2h AC | ND |
| FV520S | | EB | -70 C, 1h: PH 450 C, 2h AC | ND |
| Maraging | PH 480 C | SMA | PH 480 C, 3h AC | 2150 (310) |
| Maraging | PH 480 C | GMA | PH 480 C, 3h AC | 1290 (190) |
| Maraging | | EB | PH 480 C, 3h AC | ND |
| NCMV | T 350 C | SMA | T 350 C, 1h AC | ND |
| NCMV | | GMA | T 350 C, 1h AC | ND |
| NCMV | T 600 C | SMA | T 600 C, 1h AC | ND |

(a) ND = Not determined.

### Results of SCC Testing

*General Comments.* Table 2 gives base metal yield stress and hardness data. The toughness and SCC results obtained for the precracked samples are given in Tables 6 and 7 together with the average hardness of the region sampled in each case by the fatigue crack. Results established as being under plane strain conditions according to ASTM criteria (Ref. 8) are indicated. Most toughness and SCC tests were probably under plane strain conditions, as indicated by a general absence of shear lips on specimen fracture faces, but without measured yield stress data for the HAZ of a weld, which is difficult to obtain, this cannot be regarded as established. The stress intensity results are therefore expressed in terms of a $K_Q$ parameter. $K_Q$ is the critical stress intensity to cause failure in air when it is not known whether the test is under plane strain conditions: $K_{Qscc}$ is the corresponding SCC parameter.

While critical stress intensity criteria can be used to compare materials, the practical application of such data should make allowance for the stresses likely to arise in service. Service loading will normally be related to the base metal properties, and the $K_Q$ and $K_{Qscc}$ values obtained in Table 6 were therefore converted into defect tolerance parameters (DTPs), using the general relationships

$$DTP = [K_Q/\sigma_y]^2 \text{ or,} \quad (1a)$$

$$DTP = [K_{Qscc}/\sigma_y]^2 \quad (1b)$$

where $\sigma_y$ is the base metal yield stress (Ref. 10).

*Base Metal Behavior.* With the alloys studied and heat treatment conditions used, highest SCC resistance was shown by the FV520S and 18% Ni alloys. The RS140 and NCMV steels tempered at 600 C were comparable to these materials, but showed much greater susceptibility following tempering at 350 C. The Cu-Si alloy showed high susceptibility following heat treatment at 350 and 600 C, with relatively high hardness (550 HV) obtained even after the latter heat treatment.

*HAZ Behavior.* It is apparent from Table 6 that considerable loss in SCC resistance can occur in the as-welded transformed HAZ of a weld. This was especially the case with the medium carbon steels examined, when high hardnesses were developed as a result of the welding thermal cycle. Susceptibility to SCC was less marked with the lower carbon, low alloy and FV520S simulated HAZ samples examined. Two types of behavior within the transformed HAZ were observed, as shown in Table 7.

**Table 6 — Summary of Fracture Mechanics Results from Welds**

| Material Condition | Weld | Region tested (a) | Average Hardness HV | $K_Q$ Nmm$^{-3/2}$ (ksi$\sqrt{in.}$) | $K_{QSCC}$ Nmm$^{-3/2}$ (ksi$\sqrt{in.}$) | Defect tolerance parameter, DTP From $K_Q$ mm (in.) | Defect tolerance parameter, DTP From $K_{QSCC}$ mm (in.) |
|---|---|---|---|---|---|---|---|
| | | | **Base Metal Cu-Si** | | | | |
| T350 C | NA | BM | 560 | 1040* (30) | 244* ( 7) | 0.49 (0.02) | 0.03 (0.001) |
| T350 C | SMA | Tr HAZ | 485 | 1710 (49) | 1360 (39) | 1.32 (0.05) | 0.83 (0.03) |
| T350 C | SMA | Sub HAZ | 350 | ND | 1740 (50) | ND | 1.36 (0.05) |
| T350 C | SMA | WM | 490 | ND | 870* (25) | ND | 0.34 (0.01) |
| T350 C | NA | Sim HAZ | 709 | 975* (28) | 244* ( 7) | 0.42 (0.02) | 0.03 (0.001) |
| T600 C | NA | BM | 548 | 1640* (47) | 418* (12) | 1.44 (0.05) | 0.09 (0.004) |
| T600 C | SMA | Tr HAZ | 480 | ND | 1980 (59) | ND | 2.09 (0.08) |
| T600 C | SMA | WM | 470 | ND | 930 (27) | ND | 0.45 (0.02) |
| | | | **Base Metal RS 140** | | | | |
| T350 C | NA | BM | 590 | 1705* (49) | 418* (12) | 1.69 (0.07) | 0.10 (0.004) |
| T350 C | SMA | TR HAZ | 490 | 3270 (107) | 1170 (34) | 8.07 (0.32) | 0.79 (0.03) |
| T350 C | SMA | Sub HAZ | 425 | ND | 2750 (79) | ND | 4.41 (0.17) |
| T350 C | SMA | WM | 510 | 1950 (56) | 1370 (39) | 2.22 (0.09) | 1.09 (0.04) |
| T600 C | NA | BM | 442 | 4360 (133) | 1740* (50) | 14.4 (0.59) | 2.28 (0.09) |
| T600 C | SMA | Tr HAZ | 450 | ND | 1810 (52) | ND | 2.47 (0.10) |
| T600 C | SMA | Sub HAZ | 405 | ND | 2610 (75) | ND | 5.15 (0.20) |
| T600 C | SMA | WM | 540 | 2170 (71) | 1290* (37) | 4.6 (0.18) | 1.25 (0.05) |
| T600 C | SMA | WM[b] | 544 | 2430 (69) | 870 (25) | 4.46 (0.18) | 0.57 (0.02) |
| T600 C | EB | Tr HAZ[b] | 679 | 1870 (54) | 418 (12) | 2.64 (0.10) | 0.13 (0.005) |
| T600 C | EB | WM[b] | 641 | 1880 (54) | 630 (18) | 2.66 (0.10) | 0.32 (0.01) |
| T600 C | EB | Tr HAZ[c] | 548 | ND | 800 (23) | ND | 0.48 (0.02) |
| T600 C | NA | Sim HAZ | 692 | 1220 (35) | 244* ( 7) | 1.12 (0.04) | 0.04 (0.002) |
| | | | **Base Metal FV520S** | | | | |
| PH450 C | NA | BM | 410 | 3410 (98) | 2090* (60) | 8.94 (0.35) | 3.36 (0.13) |
| PH450 C | SMA | Tr HAZ[d] | 390 | 3480 (100) | 2720 (78) | 9.31 (0.37) | 5.70 (0.22) |
| PH450 C | SMA | Sub HAZ[d] | 410 | 3130 (90) | 2610 (75) | 7.55 (0.30) | 5.24 (0.21) |
| PH450 C | SMA | WM | 380 | ND | 2400 (69) | ND | 4.43 (0.17) |
| PH450 C | EB | Tr HAZ[d] | 405 | 4350 (130) | 2780 (80) | 15.8 (0.62) | 5.95 (0.23) |
| PH450 C | EB | WM | 255 | 4480 (129) | 2610 (75) | 15.4 (0.61) | 5.24 (0.21' |
| PH450 C | NA | Sim HAZ | 374 | 2960 (85) | 1740 (50) | 6.75 (0.27) | 2.34 (0.09) |
| | | | **Maraging Steel** | | | | |
| PH480 C | NA | BM | 408 | 3510 (101) | 2260* (65) | 8.13 (0.32) | 3.38 (0.13) |
| PH480 C | GMA | Tr HAZ | 405 | 3560 (105) | 2780 (80) | 8.81 (0.35) | 5.11 (0.20) |
| PH480 C | GMA | Sub HAZ | 410 | 3480 (100) | 2610 (75) | 8.01 (0.32) | 5.00 (0.18) |
| PH480 C | GMA | WM | 393 | ND | 2230* (64) | ND | 3.28 (0.13) |
| PH480 C | SMA | WM | 508 | 1740 (50) | 1530* (44) | 2.00 (0.08) | 1.55 (0.06) |
| PH480 C | EB | Tr HAZ | 410 | 3480 (100) | 2960 (88) | 8.01 (0.32) | 5.80 (0.23) |
| Ph480 C | EB | WM | 460 | 2090 (60) | 1390 (39) | 2.89 (0.11) | 1.28 (0.05) |
| | | | **Base Metal NCMV** | | | | |
| T350 C | NA | BM | 460 | 2020* (58) | 313* ( 9) | 1.54 (0.06) | 0.04 (0.001) |
| T350 C | GMA | Tr HAZ | 475 | 2960 (85) | 696 (20) | 3.30 (0.13) | 0.18 (0.007) |
| T350 C | GMA | WM | 350 | 2710 (78) | 2440 (70) | 2.76 (0.11) | 2.24 (0.09) |
| T350 C | SMA | WM | 520 | 1530 (44) | 139 ( 4) | 0.88 (0.03) | 0.01 (0.001) |
| T600 C | NA | BM | 430 | 3790* (109) | 1960 (56) | 10.1 (0.40) | 2.72 (0.11) |
| T600 C | SMA | Tr HAZ | 500 | ND | 1150 (33) | ND | 0.93 (0.04) |
| T600 C | SMA | WM | 570 | ND | 770 (22) | ND | 0.42 (0.02) |
| | | | **Additional Peak Hardness Studies** | | | | |
| BS968 | NA | Sim HAZ | 450 | 1570 (45) | 626* (18) | 2.03 (0.08) | 0.28 (0.01) |
| HY80 | NA | Sim HAZ | 418 | 2260 (65) | 1640* (47) | 4.27 (0.17) | 2.24 (0.09) |

(a) BM = Base Metal
Tr HAZ = transformed HAZ
Sub HAZ = subcritical HAZ
WM = weld metal
Sim HAZ = simulated HAZ
* = plane strain value

(b) As-welded
(c) Tested after T500 C, 1 h AC.
(d) Crack extended laterally and propagated in weld metal.

With the highly susceptible NCMV steel, the peak temperature reached in the HAZ had little effect on the $K_{QSCC}$, despite a considerable increase in prior austenite grain size at higher temperature. With the less susceptible HY80 alloy, increasing peak temperature and associated grain size led to reduced SCC resistance.

In multipass welds, the SCC resistance of the reheated transformed HAZ was considerably higher than in

**Table 7 — Simulated HAZ Samples: Effect of Peak Temperature**

| Steel | Peak temp. in cycling C | Sample Hardness HV | Prior austenite grain size $\mu$m | $K_{QSCC}$ Nmm$^{-3/2}$ (ksi$\sqrt{in.}$) |
|---|---|---|---|---|
| NCMV | 1300 | 622 | 100 | 520 (15) |
| NCMV | 100 | 614 | 40 | 520 (15) |
| HY80 | 1300 | 369 | 100 | 1570 (45) |
| HY80 | 100 | 368 | 25 | 2120 (61) |

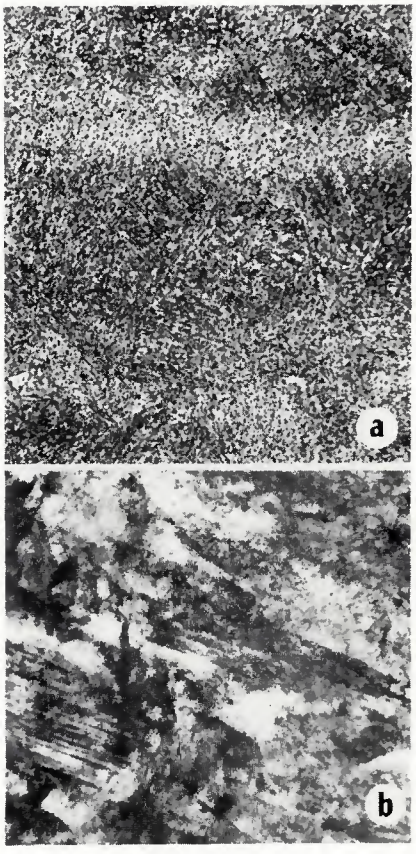


*Fig. 3 — Typical microstructures of low alloy steel base metals. (a) Cu-Si steel. X500, reduced 31%, (b) NCMV steel. X40,000 (thin foil), reduced 31%*

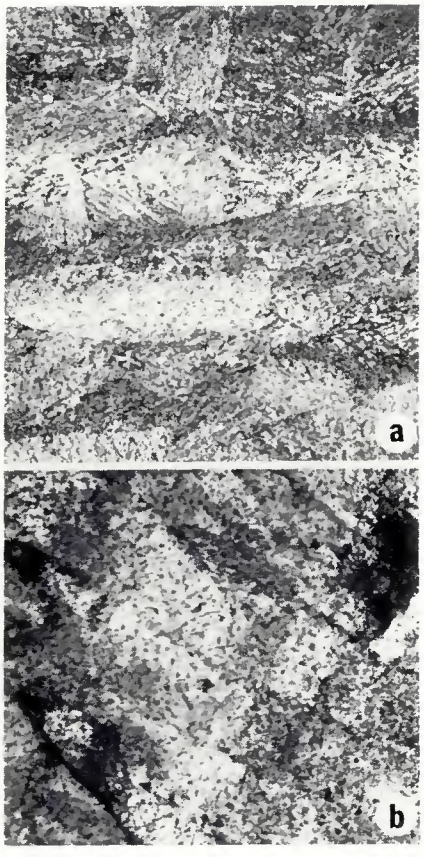


*Fig. 4 — Microstructure of maraging steel base metal (a) X500, reduced 31%, (b) X20,000 (thin foil), reduced 31%*

the as-welded condition and could exceed that of the base metals. Postweld heat treatment further improved the transformed HAZ characteristics, but the full base metal SCC resistance was obtained only when the heat treatment caused the HAZ hardness to fall to the base metal level.

All sub-critical HAZs tested showed higher SCC resistance than did the parent material.

*Weld Metal Behavior.* In most cases the matching composition weld metals studied were harder than the corresponding base metals, and showed rather higher SCC susceptibility. The exceptions to this were the FV520S EB weld, and the Cu-Si SMA weld, as both of these weld metals were appreciably softer and more resistant to SCC than the base metal. A particularly low $K_{OSCC}$ was obtained for the matching NCMV SMA weld metal tempered at 350 C, in contrast to the good resistance of the nonmatching GMA weld.

### Metallographic and Fractographic Observations

The steels studied showed three main types of microstructure. After tempering at 350 C, the medium carbon steel base metal contained twinned martensite (Fig. 3). This structure was found in the simulated HAZ samples in these alloys, and in the BS4360, although transformation in the latter material was not uniform, and intermediate transformation products were observed locally. Twinned martensite was also observed in the matching NCMV weld metal tempered at 350 C.

After heat treatment at 600 C, the medium carbon steels showed typical tempered martensite structures, with extensive carbide precipitation. Reheated transformed and subcritical HAZs and weld metals also showed this structure, apart from the matching NCMV weld metal tempered at 350 C. A fine precipitate was noted in the Cu-Si steel tempered at 600 C, this being identified as copper by electron diffraction.

The base metal and HAZ samples of the 18% Ni, FV520S and HY80 alloys all showed slipped martensites, with fine precipitation in the former two materials after postweld heat treatment. In the 18% Ni steel, the martensite appeared acicular, with occasional large martensite plates (Fig. 4). The martensite in the FV520S was in the form of largely parallel, irregular laths, while that in the HY80 was acicular (Ref. 6).

Apart from the presence of segregation of alloying elements, inclusions and austenite (Table 8), the weld metal structures were largely similar to those of the base metal with respect to martensite unit geometry and precipitation, although from visual assessment, the weld metal dislocation density was rather higher. In the low alloy steels and FV520S weld metal, segregation had little discernible effect on the distribution of precipitation following heat reatment. The maraging steel weld metals showed nonuniform precipitation, particularly in the case of the EB weld, with the density of precipitation being highest in the areas last to solidify during welding. Segregation

**Table 8 — Results of Retained Austenite Determinations**

| Material | Welding process | Austenite content % (Range)[a] | Austenite content % (Average) |
|---|---|---|---|
| Cu-Si | SMA (T 350 C) | 4.3 - 8.5 | 5.7 |
| RS140 | SMA (T 600 C) | ND[b] | ND[b] |
| RS140 | EB (As-welded) | 4.8 - 5.9 | 5.4 |
| FV520S | GTA (PH 450 C) | 16.1 - 64.1 | 20.4 |
| FV520S | EB (PH 450 C) | 43.5 - 64.1 | 53.4 |
| Maraging | SMA (PH 480 C) | 11.7 - 20.6 | 15.6 |
| Maraging | GMA (PH 480 C) | 3.2 - 5.6 | 4.4 |
| Maraging | EB (PH 480 C) | 1.6 - 17.7 | 7.2 |
| NCMV | SMA (T 350 C) | 22.2 - 34.7 | 27.3 |
| NCMV | GMA (T 350 C) | 2.4 - 4.0 | 3.2 |

(a) Range of intensities determined for $\gamma_{200}$, $\gamma_{220}$, and $\gamma_{311}$ planes relative to $\alpha_{200}$ and $\alpha_{211}$ planes.
(b) Not detected

*Fig. 5 — Microstructure of GMA maraging steel weld metal. X500, reduced 31%*

in the maraging steel weld metals was quite marked, with reverted austenite being apparent (Fig. 5). The FV520S GTA weld studied contained a very mixed microstructure, with austenite, δ ferrite and martensite being present. Considerably more retained austenite was evident in the FV520S EB weld, despite the subzero treatment used. The structure of the non-matching GMA weld in NCMV materials was predominantly a low carbon tempered bainite.

From the results in Table 6, it will be noted that there is a general trend for susceptibility to increase with increasing material hardness. Further to this, the weld and base metal samples showing highest SCC susceptibility contained twinned martensite, with only one exception, namely the Cu-Si steel tempered at 600 C. Overall, the highest SCC resistance was shown by the precipitation hardening systems, although the low alloy steels tempered at 600 C to similar hardness levels displayed broadly comparable behavior.

Three principal fracture mechanisms were observed in the high strength steels tested, namely intergranular failure with respect to prior austenite grain boundaries, and transgranular failure by cleavage or microvoid coalescence (Fig. 6) (Ref. 11). Highest SCC susceptibility was associated with intergranular failure and lowest susceptibility largely with failure by microvoid coalescece, although as the stress intensity under which cracking occurred was increased, a transition was followed from intergranular to microvoid coalescence failure.

Evidence of the solidification structure was observed on some weld metal fracture faces (Fig. 7), but there was no apparent change in fracture mechanism in such areas. In the maraging steel weld metals, it was not possible to identify any particular area of the fracture face as being related to the reverted austenite present.

## Plain Weld Studies

### Sample Preparation

Welds were selected from the prepared samples previously described to show a range of SCC behavior on the basis of fracture mechanics testing, with high and low susceptibility in various weld regions. Sections were taken from these welds, and one surface dressed flush for loading in 3 point bend, the weld reinforcement on the other surface being left intact to provide a stress concentration (Fig. 8).

In addition, welds were prepared in a lower strength steel under conditions giving hardness values in the HAZ similar to those associated with the high strength alloys, but in relatively soft base metal. For this purpose, SMA fillet welds were made in 50 mm thick steel plate to BS 4360 Grade 55E, using no preheat and austenitic stainless steel filler metal to give maximum HAZ hardness (Fig. 4a). An average HAZ hardness of 440 HV 2½ was obtained.

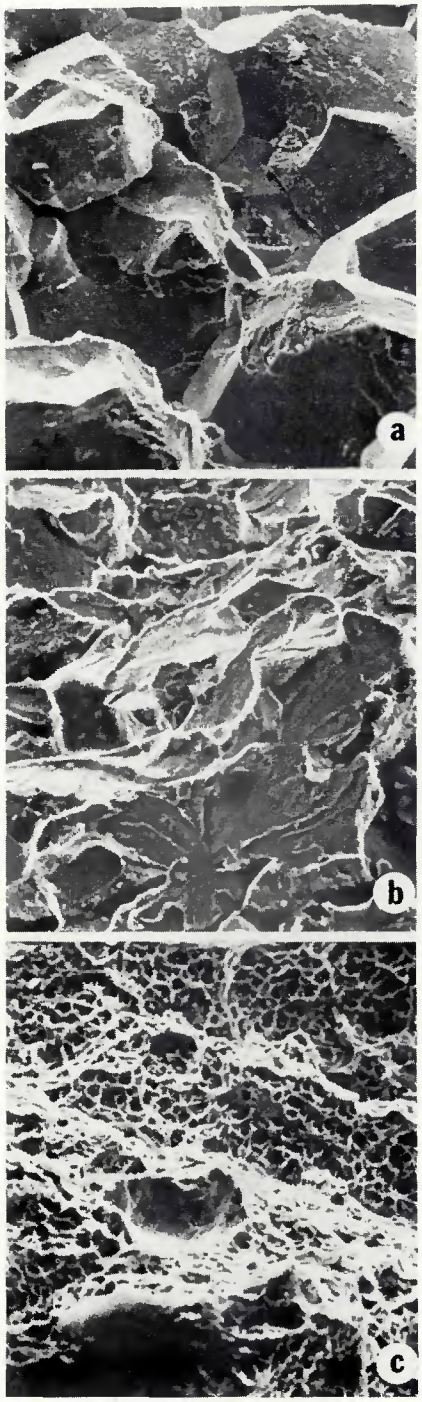


*Fig. 6 — Representative fracture faces showing principal failure mechanisms. (a) Intergranular failure (Cu-Si steel). X265, reduced 31%, (b) Cleavage failure (maraging steel). X290, reduced 31%, (c) Microvoid coalescence failure (GMA maraging steel weld metal). X500, reduced 31%*

### SCC Testing

The samples from the high strength steel butt welds were stressed in 3 point bend in 3% NaCl. Two outer fiber stress levels were studied, namely 67% and 85% of the base metal yield stress ($\sigma_y$) as representative of typical design and proof test loading respectively. The fillet weld samples were stressed in bending as in Fig. 9b, at 85% and 100% $\sigma_y$, the latter being chosen to reproduce the most severe loading likely to be encountered in practice.

The samples were left under constant load, generally until failure occurred. Test duration was noted, together with the location of failure relative to the weld.

## Results

The results obtained are summarized in Table 9, giving the applied stress level, failure time and failure location for the welds tested. DTPs derived previously for the regions where cracking initiated are given, together with the lowest DTP for any

*Fig. 7 — Evidence of the solidification structure on the fracture face of a SMA maraging steel weld metal. X60, reduced 31%*

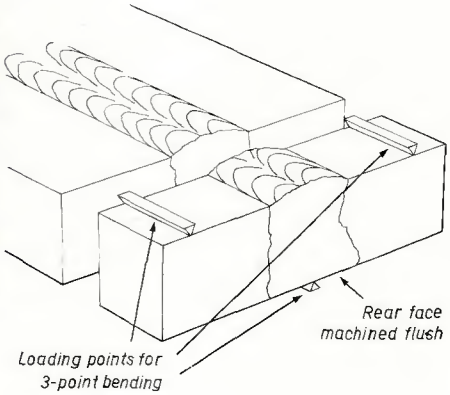


*Fig. 8 — Sketch showing sample preparation and loading points relative to weld for high strength steel butt weld samples*

**Table 9 — Results of SCC Tests on Plain Welds**

| Base Metal | Weld Process | Postweld heat treatment | Applied stress level, % $\sigma_y$ | Test duration hours | Failure region and DTP, mm (in.) | Most susceptible region and DTP mm (in.) | Critical flaw size, $a_{cr}$ from equation 2, mm (in.) Failure region | Most susceptible region |
|---|---|---|---|---|---|---|---|---|
| Cu-Si, T350 C | SMA | T350 C, 1h | 67 | 134 | WM,0.34 (0.01) | BM,0.03 (0.001) | 0.011 (0.004) | 0.02 (<0.001) |
| RS140, T600 C | SMA | None | 67 | 0.5 | WM,0.57 (0.02) | WM,0.57 (0.02) | 0.19 (0.007) | 0.19 (0.007) |
| | SMA | T600 C, 1h | 67 | 2370NF[a] | NF | WM,1.25 (0.05) | NF | 0.42 (0.02) |
| | SMA | T600 C, 1h | 87 | 1483 | WM,1.25 (0.05) | WM,1.25 (0.05) | 0.26 (0.01) | 0.26 (0.01) |
| Maraging, PH480 C | GMA | PH480 C, 3h | 67 | 3133NF | NF | WM,3.28 (0.13) | NF | 1.18 (0.04) |
| | | | 85 | 5180 | Tr HAZ,5.11 (0.02)[b] | WM,3.28 (0.13) | 1.06 (0.04) | 0.68 (0.03) |
| | EB | PH480 C, 3h | 67 | 0.01 | WM, 1.28 (0.05)[c] | WM,1.28 (0.05) | 0.43 (0.017) | 0.43 (0.03) |
| NCMV, T350 C | GMA | T350 C, 1h | 67 | 552 | Tr HAZ,0.18 (0.007) | BM,0.04 (0.001) | 0.06 (0.002) | 0.03 (0.001) |
| | SMA | T350 C, 1h | 67 | 1.3 | WM,0.01 (<0.001) | WM,0.01 (<0.001) | <0.01 (<0.001) | 0.01 (<0.001) |
| BS4360 Grade 55E | SMA | None | 85[d] | 1000NF | NF | Tr HAZ,6.81 (0.27)[e] | NF | 1.42 (0.06) |
| | SMA | None | 100[d] | 3530NF | NF | TR HAZ,6.81 (0.27) | NF | 1.02 (0.04) |

(a) NF = no failure
(b) Failure initiated in Tr HAZ, but propagated in WM.
(c) Sample contained WM crack; applied K estimated to be between 2200 and 5200 Nmm $^{3/2}$ (63-150 ksi$\sqrt{in.}$).
(d) Duplicate samples tested.
(e) $K_{OSCC}$ determined as 1040 Nmm $^{3/2}$ (30 ksi$\sqrt{in.}$).

region of each weld. These DTPs are calculated as in equation 1b above.

In addition, the fracture mechanics results were used to obtain an estimate of the size of surface defect required to cause SCC under the loading conditions used in testing the plain weld samples. For this purpose, the following relationship for a semi-elliptical surface flaw was used (Ref. 12):

$$K_{OSCC} = M_k M_s M_t M_p / \phi \cdot \sigma\sqrt{\pi a_{cr}} \quad (2)$$

where $M_k$ is a magnification factor due to the stress concentration at the weld toe;

$M_s$ $M_t$ and $M_p$ are magnification factors to correct for the free surface at the crack mouth, the free surface ahead of the crack, and the crack tip plastic zone respectively;

$\sigma$ is the remotely applied stress;

$a_{cr}$ is the critical crack depth to cause SCC, and

$\phi$ is the complete elliptic integral, its value depending on the crack front shape.

The treatment has not been rigorous in view of the uncertainty associated with appropriate $M_k$ values, and because the objective was primarily to assess the approximate size of defect that must be considered in causing SCC initiation in practice.

Equation 2 ignores any contribution to the operative stress of residual welding stresses, since in the relatively small samples used, these will have largely been relieved during machining of the specimens.

$M_k$ is dependent on the crack depth (Ref. 12), and as the crack size decreases, $M_k$ approaches the conventional stress concentration factor, $K_t$, associated with a free surface. In the present work, the crack sizes involved in initiating SCC are small in relation to the material thickness, and $M_k$ has been taken for equal to $K_t$.

Stress concentration factors reported for butt welds vary between about 1.2 and 3.0 (Ref. 13). At high stress levels, as used in the present studies some plastic deformation at the weld toe can be anticipated, and the use of stress concentration factors derived from elastic analyses should be regarded with some caution, especially the higher values reported by various workers. For the present butt welds, a $K_t$ value of 1.4 was employed, after the results of Trufyakov et al for welds stressed in bending (Ref. 14). In cases where base metal showed highest SCC susceptibility, a $K_t$ value of 1 was used to obtain a critical crack size. A number of butt weld samples failed in the weld metal, the cracks initiating at the junction between parallel weld passes. Stress concentration factors for this situation do not appear to have been investigated, and a value of 1.4 was adopted for such specimens. A factor of 1.8 was used for

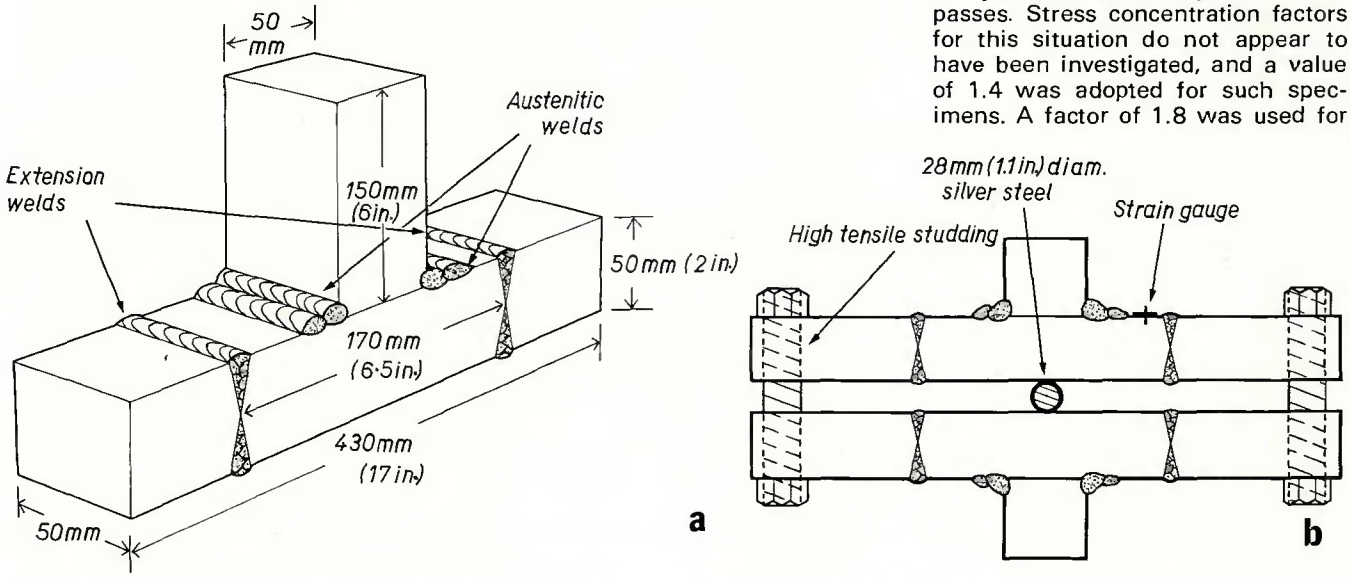


*Fig. 9 — BS 4360 Grade 55E fillet weld samples. (a) Sample geometry, (b) Loading system for SCC testing*

the fillet welds, as found by Hayes and Maddox to be applicable to a surface crack at the toe of a 30 deg fillet weld (Ref. 15), similar to the present sample geometry.

For the purpose of Table 9, it has been assumed that the initiating defect has a depth/length ratio ($a_{cr}/2c$) of 0.1, and as noted above, that $a_{cr}$ is small. Under these conditions, the term $M_s M_t M_p/\phi$ becomes 1.04 (Ref. 12).

With substitutions for the various magnification factors as indicated, equation 2 was used to calculate values of $a_{cr}$ for the weld areas where SCC occurred during test for the area defined as most susceptible by tests on precracked samples. These values are given in Table 9.

## Discussion

### Microstructure and SCC Susceptibility Relationship

The dominant role of microstructure in determining the mechanism by which SCC propagation takes place and the associated material susceptibility is well indicated by the results in Table 6. Overall, as shown by various workers, susceptibility can be expected to increase with increasing material hardness. This is illustrated by Fig. 10, which is a summary diagram prepared to include the present results and those of other investigations at The Welding Institute. Further to the effect of hardness, there is a sharp division between the high susceptibility associated with structures causing intergranular failure, and other structures. It has been suggested previously that this failure mechanism results from restriction of intragranular dislocation movement, so that the applied strain is effectively concentrated at the prior austenite grain boundaries (Ref. 11). Dislocations in twinned martensite are strongly pinned, and this phase in particular has a highly deleterious effect on SCC behavior (Refs. 6, 16). For optimum SCC performance, compositions and heat treatment conditions causing twinned martensite should be avoided. Intergranular failure can also arise in tempered martensite at high hardness levels, as shown by the Cu-Si tempered at 600 C, and it would appear that the hardness of structures other than twinned martensite should be kept below about 550 HV to obtain good SCC resistance in neutral chloride media. The relationship between material hardness and risk of SCC in service is considered further in the following.

At hardness levels below 550 HV, and in the absence of twinned martensite, susceptibility to SCC will depend largely on the ease with

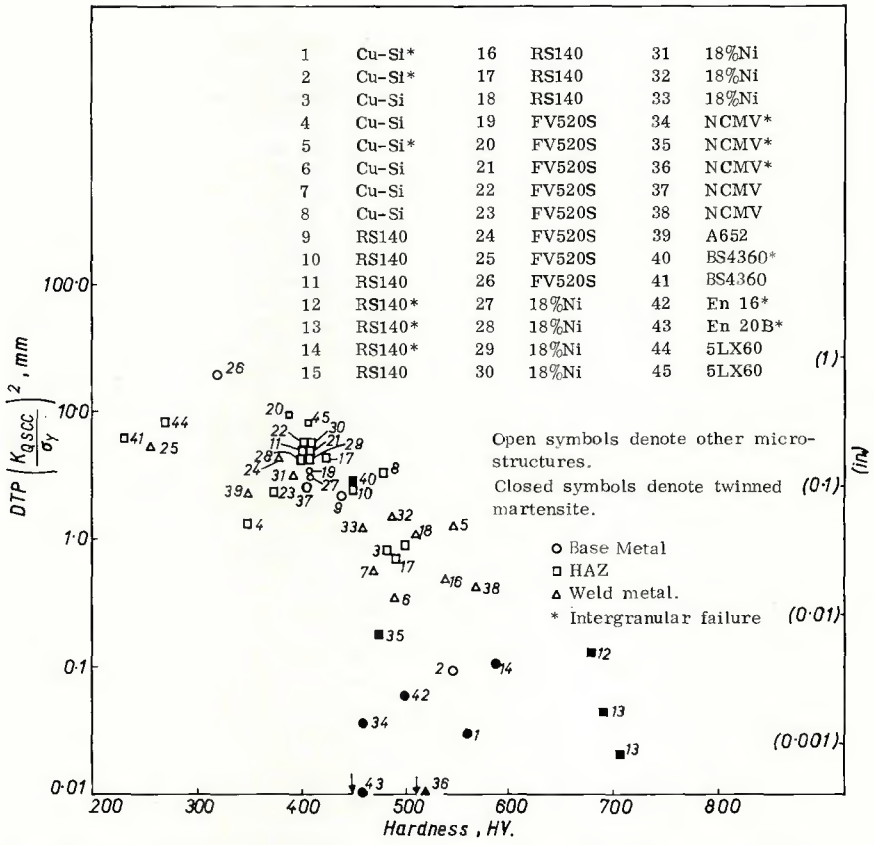


*Fig. 10 — Relationship between hardness and DTP for present and other weld samples*

which cleavage can occur. Failure by cleavage has been shown to be favored by factors such as the presence of suitable crack nucleation sites and a high material yield stress (Ref. 17). The latter is consistent with the general finding that SCC susceptibility tends to increase with increasing hardness. In respect to the former, the results in Table 6 indicate that precipitation hardened systems will afford higher SCC resistance than medium carbon alloys tempered to similar strength levels. This is likely to be due to cleavage nucleation being facilitated in medium carbon steels by the large carbide particles formed during tempering. In general, therefore, low carbon slipped massive and acicular martensites can be expected to be more resistant to SCC than tempered medium carbon martensites.

In the softer materials studied, SCC took place by microvoid coalescence. Failure by this mechanism has been found to be dependent on the density and distribution of nonmetallic inclusions, resistance to crack propagation increasing as the inclusion population is reduced (Ref. 18). Thus, the risk of SCC will be reduced by the use of cleaner material, but it must be appreciated that practical benefits from cleaner steels will largely be dependent on suppression of intergranular and cleavage failure (Ref. 11).

With lower strength steels than primarily considered in the present work, bainitic type structures may be encountered. While these have not been investigated exhaustively from the SCC viewpoint, general comments can be made from studies on hydrogen induced HAZ cracking on welding. Again, it is probable that reduction in hardness as far as possible is to be preferred, but at a given hardness level, a number of different types of bainitic or other non-martensitic structures can arise. The major point is that structures containing sheaves of parallel bainite plates should be avoided, since the resistance to cleavage may be relatively low, causing a loss of both toughness per se (Ref. 19) and resistance to hydrogen cracking (Ref. 10). Further, it is desirable to avoid transformation to structures containing intergranular pro-eutectoid ferrite surrounding an acicular intragranular structure. This structure results in applied strain being concentrated at grain boundaries analogous to the situation with twinned martensite, and a microscopically "ductile" intergranular form of cracking can result, with a marked increase in susceptibility to hydrogen induced failure (Ref. 11).

### Effects of Welding

*General Comments.* When considering the probable effects of a welding operation on the risk of SCC of a fabrication, attention should be paid to two aspects of behavior. First, the susceptibility of individual weld areas must be evaluated so that the weak link can be identified. The likelihood of cracking in service can then be assessed, and suitable remedial measures undertaken. From the present results, the performance of welded high strength steels can be expected to depend principally on the SCC resistance obtained in the transformed HAZ, and in the weld metal if this is of matching composition. Thus, particular consideration should be given to these areas in any material evaluation study.

Second, recognition must be made of the probable failure path through the welded assembly. For example, in multipass welds, softening of underlying material will occur and SCC propagation will take place into a region of reduced susceptibility, when the crack may arrest. A decision will then be necessary as to whether the crack can be tolerated, based on its probable maximum depth, or whether it will lead to failure of the fabrication by another mechanism such as fatigue.

*HAZ Behavior.* The possible deleterious effect of microstructural changes during welding is highlighted by the extreme susceptibility of the hard as-welded transformed HAZ structures developed in the medium carbon steels examined. When the transformed HAZ is sensitive in intergranular failure, the peak temperature experienced seems to have no significant effect on susceptibility, so that failure is equally likely in both the coarse and fine grain size regions of the HAZ (Ref. 21). In contrast, susceptibility to cleavage failure is affected by peak temperature, being highest in the coarse grained HAZ close to the fusion boundary. Thus, even if weld dressing is employed to remove the stress concentration at the weld toe, SCC is most likely to occur in the high temperature HAZ, and when carrying out material evaluation studies, particular attention should be paid to this region (Ref. 22). When failure occurs by cleavage, changes in welding conditions will have one of two effects (Ref. 22). With less hardenable alloys, an increase in heat input will lead to transformation on cooling to a relatively soft microstructure with low susceptibility to hydrogen embrittlement. Thus, increasing heat input will increase the SCC resistance in the transformed HAZ. With more hardenable steels, where HAZ structure is less affected by cooling rate, heat input should be minimized to reduce the extent to which grain coarsening occurs, and the width of the coarse grain HAZ region. In both situations, preheat and postweld conditions should be controlled as necessary to avoid hydrogen induced cracking during welding.

In multipass welds, the SCC behavior of the transformed HAZ is improved by the tempering effect of subsequent welding passes. The practical significance of this will depend on the heat input and thermal cycle involved in relation to the ageing characteristics of the steel, and the thermal cycle during welding may not always be adequate for HAZ resistance to equal that of the base metal. It is however noteworthy that in cases where the base metal was susceptible to intergranular failure, the reheated transformed HAZ failed by cleavage, with correspondingly high SCC resistance. The tempering effect of welding is even more marked in the subcritical HAZ regions, as in all multipass welds studied, the subcritical HAZ showed higher SCC resistance than the base metal.

*Weld Metal Behavior.* Precisely similar comments apply with respect to the effect of microstructure and hardness on SCC behavior for weld metals as for HAZs and base metals. The low alloy weld metals studied were generally harder than the base metals and HAZs, despite the multipass deposition and postweld heat treatment. This increased hardness is probably largely responsible for the weld metals showing rather higher SCC susceptibility than base metals, as indicated in Table 6.

Greatest microstructural differences between weld metal and base metal arose with the precipitation hardening alloys. The FV520S weld metals differed most with their high retained austenite contents and the presence of $\delta$ ferrite. Austenite is only slightly sensitive to hydrogen embrittlement, and the high SCC resistance of these weld metals may well be due in part to the retained austenite, especially in the soft EB weld metal. Certainly, the austenite would tend to retard crack propagation, and may be of further benefit by acting as a "sink" for hydrogen formed during corrosion. Toy and Philips showed that hydrogen may be picked up by reverted austenite in maraging steel weld metals, with an associated strain-induced transformation to martensite (Ref. 23), and they suggested that the SCC susceptibility of such weld metals is due to the austenite present. This is unlikely to be entirely correct, since base metal containing negligible amounts of austenite suffers SCC, while if austenite were dominant in causing failure, the present maraging steel SMA weld metal should have a much lower $K_{OSCC}$ than the other maraging steel weld metals, (Table 9), and this was not the case. It is therefore probable that Toy and Philips' observations are an effect of SCC rather than a cause, and austenite should be regarded as beneficial in improving SCC resistance.

It might be expected that local compositional variations arising from segregation would affect weld metal SCC behavior. To some extent, this appears to be true in that evidence of the solidification structure was observed on some fracture faces. However the association between fracture path and segregation was not marked, and segregation does not seem to play a major role in determining SCC resistance. Segregation may be of more significance in precipitation hardening systems than in low alloy steels, as indicated by the nonuniform precipitation observed in the maraging steel EB weld metal. This weld metal gave low $K_Q$ and $K_{QSCC}$ values relative to the GMA weld, for example. It has been reported previously that EB welds in this type of steel have poor fracture toughness, although the reason has not been clear (Ref. 24). However, segregation of hardening elements during solidification will affect the local response of the weld metal to the precipitation hardening heat treatment, and a deterioration in mechanical properties would not be unexpected. Such an effect will be particularly marked in EB weld metal, since the high solidification rates experienced with this process will promote segregation of alloying elements.

The presence of deoxidation products and other inclusions in weld metals will reduce SCC resistance to some extent, and this may have contributed to the low weld metal $K_{QSCC}$ values observed. However, as previously pointed out, inclusions are of most importance in affecting crack propagation by microvoid coalescence. Most of the present weld metals failed largely by cleavage. Hence although a reduction in inclusion content is presumably of benefit with respect to weld metal SCC behavior, inclusions are likely to be of secondary importance compared to microstructure.

### Postweld Heat Treatment

A salient feature of the present results is that given postweld heat treatment similar to that applied to base metal, there was no loss in SCC resistance in the weld area, provided only that the final hardness was near the base metal level. This proviso was not fulfilled with the low alloy weld

metals, nor with the transformed HAZ of the NCMV steel tempered at 600 C. Nonetheless, the results show that postweld heat treatment should be regarded as essential to obtain maximum SCC resistance from welded joints in high strength steels.

### Correlation Between Fracture Mechanics Data and Plain Weldment Behavior

The results in Table 9 show the plain welds to have behaved largely as predicted from consideration of the fracture mechanics data. The welds found to have the longest lives were those with the highest DTPs, while failure generally took place in the area established as most susceptible from the precracked specimen studies.

In the NCMV GMA and Cu-Si SMA welds, the lowest DTP was that of the base metal, yet SCC took place in the weld region. This variation however, is not surprising in view of the very low DTPs, for these steels; minor surface irregularities will be sufficient to cause SCC, and initiation from the rough, as deposited, weld metal must be regarded as at least as probable as initiation in the base metal.

Severe localized weld toe pitting was noted with the maraging steel GMA weld stressed at 85% $\sigma_y$, SCC taking place from an elongated pit of about 1.5 mm (0.06 in.) depth. This pit depth would be expected to cause failure, being greater than the critical flaw sizes derived for the weld metal and HAZ of 0.68 and 0.06 mm (0.03 and 0.04 in.) respectively, although the stress intensity associated with a pit will presumably be somewhat less than with the sharp planar defect geometry assumed in equation 2. No comparable localized attack was found on any alloy steel tested, only general pitting being observed.

The RS140 SMA weld which was not heat treated after welding beyond maintenance of the 250 C preheat showed failure initiating between the two final passes of filler metal. These had not benefited from tempering during multipass deposition, and were considerably harder (~620 HV) than the balance of the weld metal (~540 HV), and thus presumably more susceptible to SCC. This demonstrates the danger of retaining hard untempered material in the weld area, since despite the relatively high DTP for the reheated weld metal, failure occurred after only 0.5 h.

Overall, it may therefore be concluded that the results shown in Table 9 confirm the validity and usefulness of the fracture mechanics approach adopted to define relative material SCC behavior, and the effects of welding. Thus, comparative data derived from laboratory studies on precracked specimens may be used to assess the probable service performance of a welded joint. The principal limitation to this is likely to arise with high alloy materials, where marked pitting corrosion in the weld area may occur, with an associated risk of failure (Ref. 6).

### Effect of Weld Toe Stress Concentration on SCC Initiation

The practical effects of static and dynamic strain on the corrosion of ferritic steels have not been unambiguously defined. However, even though the corrosion rate may be increased in some conditions by tensile strain, as will be experienced at a weld toe, available data suggest that strain will have little effect on the long term corrosion of low alloy steels in neutral chloride media (Ref. 26). This is certainly indicated by the lack of preferential weld toe attack with the present low alloy materials. The effective anode area/cathode area ratio of the weld toe and base metal may affect the situation to some extent, but it is considered that the present samples were sufficiently large for their anode area/cathode area ratio to adequately reproduce the practical case.

It should nonetheless be appreciated that the pitting corrosion involved in SCC initiation is to some degree autocatalytic, and as a general principle, any local increase in corrosion rate due to tensile strain at a surface irregularity will tend to be concentrated. Unless stifled by corrosion product, therefore, the development of a pit suitable for SCC initiation is more likely at a weld toe than at a plane surface. The practical significance of this effect will depend on the corrosion conditions engendered by the material/microstructure/environment combination being considered. As noted earlier, such local attack was observed in a maraging steel GMA weld, and it is probable that the effect will be of greater significance with high alloy materials which may be sensitive to pitting attack than with low alloy steels. It is not possible to make any quantitative prediction at the present time, but it can be expected that SCC resistance in high alloy weldments can be improved by dressing the weld to remove the reinforcement and obtain a plane surface.

### Practical Risk of SCC

It will be appreciated from Tables 6 and 9 that susceptibility of high strength steels to SCC is associated with relatively low DTPs and critical flaw sizes, and the question arises as to what level of DTP is acceptable for practical purposes. In the first instance, this will depend on the limits of detection afforded by nondestructive testing (NDT). However, from the magnitude of the flaw sizes derived, all materials studied must be regarded as potentially susceptible to SCC with normal NDT methods. Changes in the values of stress magnification factor and flaw shape parameter used in equation 2 to allow for different practical situations are unlikely to more than double the critical flaw sizes given in Table 9, even accepting that precise analyses are not presently available for small surface flaws. Thus it will not always be possible to guarantee avoidance of pre-existing defects of critical size by NDT. Even with sufficiently sensitive NDT, it is not possible to be specific regarding an acceptable DTP for a given service duty, since this will depend on the service environment with respect both to the amount of hydrogen taken up by the steel, and to the likelihood of SCC initiation by pitting corrosion.

Nonetheless, it should be possible to define acceptable materials for different service conditions by obtaining an empirical correlation between laboratory test data and direct practical experience. It has been suggested that consideration should be given to the concept of a critical hardness below which SCC does not occur in a given medium (Ref. 6). The approach is analogous to that used in designing welding procedures for structural steels, in giving a parameter which effectively describes the situation where the risk of cracking is controlled to a negligibly low level under the combined effect of operative stress, size of any discontinuity, hydrogen content and microstructure likely to be encountered in practice.

Without more data on the hydrogen producing potential of different media than are presently available, very few points can be located on such a critical hardness scale. However, it is well established that sour oil or gas media represent a severe case, since the sulphide scale formed by corrosion tends to poison the hydrogen evolution reaction and cause high material hydrogen contents (Ref. 5). In such duties, failure can take place at above about 240 HV, and in view of the severity of the environment this hardness can, for most practical purposes, be regarded as a lower boundary with respect to SCC arising from hydrogen embrittlement.

Further, Bloom showed that in marine conditions, martensitic stainless steels are unlikely to fail by SCC at below 400 HV, while in a salt fog or industrial atmosphere, a hardness of 450 HV could be tolerated (Ref. 27). These materials may be considered a severe case insofar as they are likely

to suffer marked pitting corrosion, and it is probable that susceptibility at hardnesses below 400 HV will not be significant in marine conditions. Certainly the results in Table 9 are in accordance with this, although some caution is necessary, in that at 400 HV, the steels may be sensitive to defects about 1 mm deep (cf Fig. 10 and Table 6): the sustained rate of pitting of low alloy steels in seawater can approach 0.7 mm/yr. (Ref. 28), and the risk of long term SCC initiation must not be overlooked. The critical figure of 400 HV is almost certainly conservative for typical offshore applications involving C-Mn and similar low alloy structural steels, where the service stress levels will be lower than with high strength steels. This is indicated by the absence of cracking in the BS 4360 fillet welds tested (Table 9), and by the fact that the Welding Institute investigators have not observed any service SCC failure in structural steelwork exposed to marine conditions, even though hardnesses approaching 450 HV must have existed in some situations. It is therefore considered that a critical hardness of 450 HV should be regarded as applicable to offshore structural steelwork. Service failures have been observed in rather higher strength alloys than C-Mn structural steels at above 400 HV when cathodically protected by zinc, and the possible adverse effect of cathodic polarization and concomitant hydrogen formation upon data shown in Fig. 10 must be borne in mind.

## Conclusions

1. The SCC susceptibility of high strength steels may be greatly increased by welding, especially if marked hardening occurs in the HAZ or weld metal as a result of the weld thermal cycle.

2. If postweld heat treatment is applied so that the hardness of the weld area is restored to that of base metal, there will be no significant loss in SCC resistance of the assembly. If such heat treatment is not applicable, increased susceptibility must be anticipated in the transformed HAZ, and in matching composition weld metal.

3. The susceptibility of welded high strength steels to SCC is primarily dependent on the microstructure produced in the different weld areas. Susceptibility generally increases with increasing hardness, while the presence of twinned martensite in particular is deleterious.

4. SCC can take place intergranularly with respect to prior austenite grain boundaries, or in a transgranular manner by cleavage or microvoid coalescence. Highest susceptibility arises with intergranular failure.

5. With the particular alloys studied, highest SCC resistance was found with low carbon precipitation hardening materials. If tempered at high temperature to similar hardness levels, medium carbon low alloy grades will be generally comparable with precipitation hardening systems, and the former materials may be preferable if marked pitting attack is likely in service.

6. The presence of alloy element segregation and inclusions may reduce the SCC resistance of high strength steel weld metal, but such effects are of secondary importance compared with that of microstructure. The adverse effect of segregation may be most marked in high alloy precipitation hardening steels.

7. The stress concentration at a weld toe does not significantly affect the corrosion processes causing SCC initiation in low alloy steels in neutral chloride media. Such stress concentrations can, however, localize attack in high alloy materials and promote SCC initiation at the weld toe. Thus, while fracture mechanics tests can be used to give comparative data on resistance to crack propagation, conventional tests on uncracked samples are essential to define the risk of SCC initiation taking place by a corrosion mechanism in service.

8. Consideration has been given to the risk of SCC in different environmental conditions. Other work has indicated that SCC in marine conditions will not occur in material softer than 400 HV: the present results on high strength steels are in accordance with this finding. However, it is considered that this critical hardness is conservative for structural steels where the service stresses are lower than with high strength alloys; test results and practical experience indicate that SCC is unlikely in structural steels at below 450 HV when exposed to marine conditions.

*Acknowledgements*

The work carried out was jointly funded by The Welding Institute and RARDE. Acknowledgement is also made to RARDE for supplying the experimental steels.

The writer thanks Mr. G. Regelous for his organization of the experimental work, and Messrs. B. Ginn, D. Boud, R. Gant and M. Catling for their experimental assistance.

*References*

1. Evans, U. R., *The Corrosion And Oxidation of Metals,* Edward Arnold (Publishers) Ltd., London, 1960.

2. Shatt, H. J. and Phelps, E. H., "Effect of Solution pH on the Mechanism of Stress Corrosion Cracking of a Martensitic Stainless Steel", *Corrosion,* 17, (9), 1961, 430t-434t.

3. Barth, C. F. Steigerwald, E. A., and Troiano, A. R., "Hydrogen Permeability and Delayed Failure of Polarized Martensitic Steels", *Corrosion,* 25 (9), 1969, pp 353-358.

4. Gooch, T. G., McKeown, D. and Willingham, D., "Stress Corrosion of Welded Materials: Evaluation and Control", *Metal Construction and British Welding Journal,* 1 (10), 1969, pp 469-475.

5. Phelps, E. H., "A Review of the Stress Corrosion Behavior of Steels with High Yield Strength", *Proc. Conf. "Fundamental Aspects of Stress Corrosion Cracking",* Ohio State University, NACE, 1967, pp 398-410.

6. Gooch, T. G., "Stress Corrosion of Welded High Strength Steels", *Welding Research International,* 3 (2), 1973, pp 17-43.

7. Brown, B. F., "The Application of Fracture Mechanics to Stress Corrosion Cracking". *Metallurgical Review,* No. 129, 1969.

8. ASTM STP "Fracture Toughness Testing and Applications" No. 381, 1965, and "Plane Strain Crack Toughness Testing of High Strength Metallic Materials". No. 410, 1967.

9. Gooch, T. G., "Stress Corrosion Testing of Welded Joints", *AGARD Conference Procedings No. 98. "Specialists Meeting on Stress Corrosion Testing Methods",* NATO, 1972, Paper 10.

10. Burdekin, F. M. and Dawes, M. G., "Practical Use of Linear Elastic and General Yielding Fracture Mechanics with Particular Reference to Pressure Vessels", *Proc. Conf. "Application of Fracture Mechanics to Pressure Vessel Technology"* I Mech. E., London, 1971, pp 28-37.

11. Gooch, T. G. and Cane, M. W. F., "Fractographic Observations of Hydrogen Induced Cracking In Steel", *Proc. Conf. "The Practical Implications of Fracture Mechanisms",* Newcastle, Institution of Metallurgists, 1973, pp 95-102.

12. Maddox, S. J. "An Analysis of Fatigue Cracks in Fillet Welded Joints", to be published in *International Journal of Fracture.*

13. Gurney, T. R. *Fatigue of Welded Structures,* Cambridge University Press, Cambridge 1968.

14. Trufyakov, V. I., Osaulenko, L. L. and Koryagin, "Stress Concentration in Butt Joints", *Automatic Welding,* 19 (10), 1966, pp 18-21.

15. Hayes, D. J. and Maddox, S. J., "The Stress Intensity Factor of a Crack at the Toe of a Fillet Weld", *The Weld Inst. Res. Bulletin,* 13 (1), 1972, pp 15-17.

16. Snape, E., "Sulphide Stress Corrosion of Some Medium and Low Alloy Steels", *Corrosion,* 23 (6), 1967, pp 154-172.

17. Knott, J. F. "Second-Phase Particles and the Toughness of Structural Steels", *Proc. Conf. "Effect of Second Phase Particles on the Mechanical Properties of Steel,* Scarborough, I.S.I., 1971, pp 44-53.

18. Steele, A. C. "The Effects of Sulphur and Phosphorus on the toughness of Mild Steel Weld Metal", *Welding Research International,* 2 (3), 1971, pp 37-76.

19. Dolby, R. E. and Knott, J. F. "Toughness of Martensitic and Martensitic-Bainitic Microstructures with Particular Reference to Heat Affected Zones in Welded Low-Alloy Steels", *J. Iron and Steel Inst.,* 210 (11), 1972, pp 857-865.

*(Continued on p. 306-s)*